

Evaluation of intervertebral disc regeneration with implantation of bone marrow mesenchymal stem cells (BMSCs) using quantitative T2 mapping: a study in rabbits

Feng Cai · Xiao-Tao Wu · Xin-Hui Xie · Feng Wang ·
Xin Hong · Su-Yang Zhuang · Lei Zhu · Yun-Feng Rui ·
Rui Shi

Received: 6 June 2014 / Accepted: 24 July 2014 / Published online: 13 August 2014
© SICOT aisbl 2014

Abstract

Purpose The aim of the study was to investigate the curative effects of transplantation of bone marrow mesenchymal stem cells (BMSCs) on intervertebral disc regeneration and to investigate the feasibility of the quantitative T2 mapping method for evaluating repair of the nucleus pulposus after implantation of BMSCs.

Methods Forty-eight New Zealand white rabbits were used to establish the lumbar disc degenerative model by stabbing the annulus fibrosus and then randomly divided into four groups, i.e. two weeks afterwards, BMSCs or phosphate-buffered saline (PBS) were transplanted into degenerative discs (BMSCs group and PBS group), while the operated rabbits without implantation of BMSCs or PBS served as the sham group and the rabbits without operation were used as the control group. At weeks two, six and ten after operation, the T2 values and disc height indices (DHI) were calculated by magnetic resonance imaging (MRI 3.0 T), and the gene expressions of type II collagen (COL2) and aggrecan (ACAN) in degenerative discs were evaluated by real-time reverse transcription polymerase chain reaction (RT-PCR). T2 values for the nucleus pulposus were correlated with ACAN or COL2 expression by regression analysis.

Results Cell clusters, disorganised fibres, interlamellar glycosaminoglycan (GAG) matrix and vascularisation were observed in lumbar degenerative discs. BMSCs could be found

to survive in intervertebral discs and differentiate into nucleus pulposus-like cells expressing COL2 and ACAN. The gene expression of COL2 and ACAN increased during ten weeks after transplantation as well as the T2 signal intensity and T2 value. The DHI in the BMSCs group decreased more slowly than that in PBS and sham groups. The T2 value correlated significantly with the gene expression of ACAN and COL2 in the nucleus pulposus.

Conclusions Transplantation of BMSCs was able to promote the regeneration of degenerative discs. Quantitative and non-invasive T2 mapping could be used to evaluate the regeneration of the nucleus pulposus with good sensitivity.

Keywords Bone marrow mesenchymal stem cells · Intervertebral disc degeneration · T2 mapping · Quantitative analysis · Aggrecan · Type II collagen

Introduction

It is well known that lower back pain is one of the most common orthopaedic diseases. The annual health costs between US\$19.6 and US\$118.8 billion in the USA were attributable either directly or indirectly to lower back pain, about 20 % of which was caused by intervertebral disc degeneration (IVDD) [1]. Current treatments for lumbar disc degeneration include non-operative approaches and surgery such as discectomy and spinal fusion. The shortcoming of these treatments was that the function of the intervertebral disc (IVD) could not be preserved [2]. Moreover, surgery reduced the mobility of spinal segments and increased the mechanical load and stress on adjacent discs [3].

Mesenchymal stem cells (MSCs) or multipotent stromal cells are non-haematopoietic progenitor cells that can differentiate into multiple cell lineages including adipogenic,

F. Cai · X.-T. Wu (✉) · X.-H. Xie · F. Wang · X. Hong ·
S.-Y. Zhuang · L. Zhu · Y.-F. Rui · R. Shi
Department of Orthopedics, Zhong Da Hospital,
Southeast University, Nanjing, China
e-mail: wuxiaotao@medmail.com.cn

X.-H. Xie (✉)
Department of Orthopedics, The First Affiliated Hospital of
Soochow University, Suzhou, China
e-mail: xiexinghuixh@163.com

osteogenic and chondrogenic cells [4–6]. Recent studies have shown that bone marrow mesenchymal stem cell (BMSC)-based therapy was effective in the treatment of IVDD by histological grading, immunohistochemistry and Western blotting. Though the data yielded by these methods are valid and reliable, they cannot be used for clinical evaluation because of their invasive nature. It is important for us to translate the laboratory findings or methods to clinical application according to the requirements of translational medicine [7]. So it is necessary to find a non-invasive and effective way to measure the biological effects of IVDD treatment and facilitate future clinical application.

The main pathological change in IVDDs was the degradation of the extracellular matrix including aggrecan (ACAN) and type II collagen (COL2) [8]. ACAN provides intervertebral discs with the ability to resist compressive loads, while COL2 confers tissue shape and tensile strength. Localised high concentrations of ACAN provide the osmotic properties necessary for normal tissue function. ACAN produces swelling pressure that counters the compressive loads on the tissue through their interaction with water. This function is dependent on a high ACAN concentration present in the extracellular matrix [9]. Synthesis and degradation of the extracellular matrix are investigated for their important roles in the IVD during disc degradation and aging [10].

It is known that increased matrix synthesis indicates disc regeneration after BMSC transplantation [11, 12]. In this study, we aimed to develop a non-invasive and practical measure for monitoring increases in disc matrix content such as ACAN and COL2.

Magnetic resonance imaging (MRI) is a non-invasive procedure commonly used in the clinical setting. T2 signal intensity is widely used to estimate the degenerative changes in IVDs. However, T2 signal intensity is affected by many factors such as the pulse sequence, type of scanners and various image parameters, so it is hardly possible to obtain stable values of signal intensities for comparison. Unlike the signal intensity, T2 relaxation time is the decay constant of MRI T2 signal intensity and neither scanner nor image parameter dependent. T2 relaxation time is an intrinsic property of tissue, reflecting the molecular environment therein, especially the water content. It is known that T2 relaxation time is positively correlated with both the proteoglycan and water content of IVDs [13–16]. The water content of the nucleus pulposus depends principally on the concentration of glycosaminoglycan (GAG), which is the primary component of ACAN. Thus, T2 mapping is indicative of the nucleus pulposus changes occurring in the early stages of IVDD [16–18]. T2 mapping has a high potential for non-invasive assessment of the nucleus pulposus and cartilage and was used in many studies because of its ability to quantify biochemical tissue characteristics [13–16, 19–22].

To our knowledge, quantitative T2 mapping has not yet been used in evaluation during regeneration of the nucleus pulposus after BMSC transplantation. Therefore, the objective of this study was to explore the curative effects of BMSC transplantation on intervertebral disc regeneration and to investigate the feasibility of the quantitative T2 mapping method for evaluating repair of the nucleus pulposus after implantation of BMSCs.

Methods

Laboratory animals and groups

All experiments were conducted with the approval of the Animal Care and Use Committee of Southeast University, Nanjing, China. Forty-eight adult New Zealand white rabbits (Jiangsu Academy of Agricultural Sciences) weighing 2.0 kg were randomly divided into four groups: BMSCs or phosphate-buffered saline (PBS) were transplanted into degenerative discs (BMSCs group and PBS group); the rabbits with operation but without implantation of BMSCs or PBS served as the sham group and the rabbits without operation used as the control group.

Isolation and culture of autologous BMSCs

The bone marrow was aspirated with 10-ml syringes that were rinsed with 1,000 units of heparin. The 5 ml of bone marrow obtained from each iliac crest was collected and mixed with an equal volume of PBS. BMSCs were isolated from the marrow aspirate by gradient centrifugation for 30 minutes at room temperature, using Ficoll-Paque PLUS (1.077 g/ml, GE Healthcare Life Sciences) as reported previously [23]. Cells were cultured in Dulbecco's modified Eagle's medium with low glucose (DMEM-LG, Gibco, Invitrogen, Carlsbad, CA, USA), supplemented with 10 % (v/v) fetal bovine serum (FBS, Wisent Inc., St-Jean-Baptiste, QC, Canada) and incubated at 37 °C in a humidified atmosphere containing 5 % CO₂ with regular replenishment of medium every two to three days. Cells were digested by 0.05 % trypsin/ethylenediaminetetraacetate (EDTA) (Gibco, Invitrogen, Carlsbad, CA, USA) upon 80–90 % confluence and subcultured as passage 1 (P1).

Differentiation of BMSCs

Osteogenic differentiation: BMSCs at P3 were trypsinised and cultured in six-well culture plates at a concentration of 2×10^3 cells/cm². The osteogenic induction medium contained 10 % (v/v) FBS, 100 nM dexamethasone (Sigma, St. Louis, MO, USA), 10 mM beta-glycerophosphate (Sigma) and 0.05 mM ascorbic acid (Sigma) in DMEM with high glucose. The

medium was changed every three days. The osteogenic differentiation of the cells was detected by staining for calcium nodules, using 2 % Alizarin Red S at four weeks after induction.

Adipogenic differentiation: BMSCs at P3 were trypsinised and cultured in six-well culture plates at a concentration of 2×10^3 cells/cm². The adipocyte induction medium contained 10 % (v/v) FBS, 1 μ M dexamethasone, 200 μ M indomethacin (Cyagen, Guangzhou, China), 0.5 mM 3-isobutyl-1-methyl-xanthine (IBMX, Cyagen) and 10 μ g/ml insulin (Cyagen). The medium was changed every three days. Cells differentiated into adipocytes were identified by staining with Oil Red O at four weeks after induction.

Chondrogenic differentiation: BMSCs (2.5×10^5 cells) were placed into 15-ml polypropylene tubes and centrifuged for five minutes at 1,500 rpm until a three-dimensional cell pellet developed. The chondrogenic induction medium was gently added; the medium contained 10 nM dexamethasone, 10 ng/ml transforming growth factor, beta 3 (TGF- β_3 , Cyagen), 50 mg/ml ascorbic acid (Sigma) and 50 mg/ml ITS+Premix (Cyagen) in DMEM with high glucose. The tubes were incubated at 37 °C in a humidified atmosphere under 5 % (v/v) CO₂. Medium changes were made every three days for four weeks. Pellets were formalin-fixed and frozen-sectioned (thickness: 8 μ m) for Alcian Blue staining.

Establishment and evaluation of the IVDD model in rabbits

Lumbar IVDD was induced in rabbits by stabbing the annulus fibrosus (AF) as previously described [24]. Briefly, under general anaesthesia, the left anterolateral vertebral column from L3 to L6 was exposed via a retroperitoneal approach. The L3–L4, L4–L5 and L5–L6 lumbar IVDs were stabbed with a 20-gauge hypodermic needle to a depth of 5 mm in the left anterolateral AF (Fig. 1) and surgical wounds were routinely closed. The spine of the rabbits was scanned using 3.0-T MRI 2 weeks after stabbing.

Two weeks after model establishment, one test animal and one normal animal were euthanised by intravenous injection of high-dose pentobarbitone sodium (120 mg/kg) (Sigma). The L3–L4, L4–L5 and L5–L6 discs were excised immediately, together with the cranial and caudal vertebral bodies. Then the vertebral body-disc-vertebral body units were fixed in 10 % (v/v) formalin in neutral buffer, decalcified in 10 % (w/v) EDTA, dehydrated in a graded series of ethanol baths (70, 90 and 99 %, all v/v) and individually processed after paraffin embedding. Paraffin blocks were sectioned transversely, using a microtome (thickness: 4 μ m). Sections were stained with haematoxylin and eosin (H&E).

Transplantation of BMSCs

Cultured BMSCs at P3 were transplanted into degenerative discs at L3–L4, L4–L5 and L5–L6 in anaesthetised rabbits

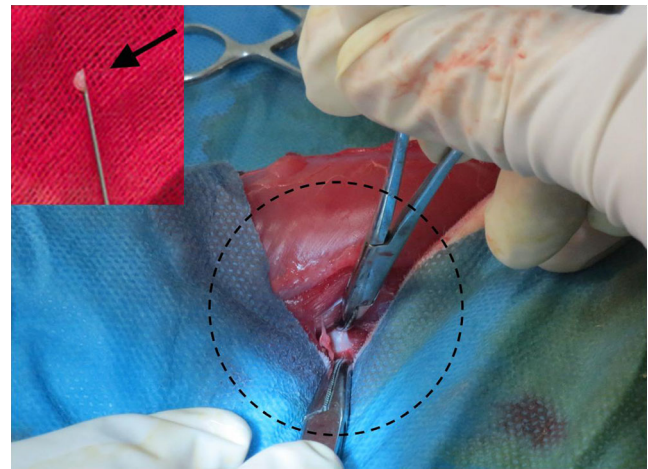


Fig. 1 Lumbar IVDD was induced in all rabbits by stabbing the annulus fibrosus. The front edge of annulus fibrosus was explored and then released from the needle shown in the *upper left* (arrow)

two weeks after stabbing. BMSCs were diluted in PBS to 1×10^6 cells/ml, and 20- μ l amounts of cell suspension were carefully injected into each disc through a 27-gauge insulin microinjector.

MRI evaluation

MRI examinations were performed using a 3.0-T MRI unit (Verio 3.0 T MR, Siemens Medical Solutions, Erlangen, Germany) at weeks two, six and ten after transplantation. Rabbits were placed supine on a quadrature surface coil and sagittal images were obtained through the lumbar spine, with detailed parameters summarised in Table 1.

All images were evaluated by two radiologists for consensus. One had more than six years relevant experience and a special interest in musculoskeletal radiology, and the other had more than ten years experience in musculoskeletal radiology. Assessment was performed using region of interest (ROI) analysis. ROIs were delineated in the area of the nucleus pulposus and were required to cover the entire nucleus when T2 relaxation time was evaluated.

The disc height index (DHI) of Lu et al. [25] was calculated to allow comparisons between groups. Changes in the DHI were expressed as %DHI values and normalised to measured preoperative IVD heights (%DHI = postoperative DHI / preoperative DHI \times 100 %) (Fig. 2).

Real-time reverse transcription polymerase chain reaction (RT-PCR) for evaluating the expression of matrix-specific genes of the nucleus pulposus

After MRI examination, rabbits were killed by intravenous injection of an overdose of phenobarbitone sodium (120 mg/kg, Sigma). The L3–L4, L4–L5 and L5–L6 discs were excised immediately, in continuity with their cranial and

Table 1 MRI parameters

Sequence	T1w FSE sagittal	T2w FSE sagittal	T2 map sagittal
Slices	11	11	11
Field of view	140×140 mm	140×140 mm	140×140 mm
Slice thickness	2.0 mm	2.0 mm	2.0 mm
TR/TE	722/11	3,000/102	4,000/10,122,234
Average	9	9	8
Image matrix	288×384	288×384	240×320
Echo trains/slice	5	21	11

T1w FSE T1-weighted fast spin echo sequence, *T2w FSE* T2-weighted fast spin echo sequence, *TR* repetition time, *TE* echo time

caudal vertebral bodies. The columnar tissues were removed, as were muscles and nerves, and the vertebral body-disc-vertebral body units were separated and stored in liquid nitrogen.

Real-time RT-PCR was used to analyse the expression of *COL2* and *ACAN*. Total RNAs were isolated from L3–L4, L4–L5 and L5–L6 nucleus pulposus immediately after separation. Briefly, each nucleus pulposus was minced using a sterile scalpel, snap-frozen and pulverised in liquid nitrogen. The tissue powder was homogenised with the Isogen reagent (TaKaRa, Otsu, Shiga, Japan) according to the manufacturer's instructions. RNA samples were then reverse-transcribed into cDNA using PrimeScript® First Strand cDNA Synthesis Kits (TaKaRa).

Real-time quantitative PCR using gene-specific primers (Table 2) was performed on cDNA derived from nucleus pulposus samples employing the SYBR Green method, as previously described. Reactions were conducted on a 7,300 Real-Time PCR System (Applied Biosystems, Foster City, CA, USA), in triplicate, in 96-well plates in final volumes of

20 µl, under standard conditions. Reaction mixes contained 10 µl 2× SYBR Green Mastermix (TaKaRa), 0.4 µl (10 µM solution) forward primer, 0.4 µl (10 µM solution) reverse primer, 0.4 µl ROX Reference Dye (50×), 6.8 µl water and 2 µl (5 ng/µl) cDNA. The $2^{-\Delta C_t}$ and $2^{-\Delta\Delta C_t}$ methods were used to calculate the relative expression levels of target genes. The housekeeping gene GAPDH was used as a reference to normalise PCR data, expressed as gene of interest to GAPDH ratios.

Statistical analysis

Statistical analysis was performed using SPSS 20.0 software. All values were presented as means±SD. The one-way analysis of variance (ANOVA) was used to compare the results among the four groups and regression analysis was used to reveal the correlation between T2 value and matrix expression. *P* values less than 0.05 were considered statistically significant.

Results

Characteristics of BMSCs

P3 cells were incubated for 28 days in the presence of agents triggering specific differentiation into osteoblasts, chondrocytes and adipocytes. The results showed that the expanded cells were BMSCs, which maintained their phenotype to differentiate into multiple cell types (Fig. 3).

Evaluation of the IVDD model

In the control group, cells were distributed regularly in the nucleus pulposus. Single cells or islets composed of a few chondrocyte-like cells (surrounded by a capsule) were evident among sparse collagen fibres, and cell clusters were absent under the microscope. Regularly collagen-rich lamellae with fibrochondrocytes could be found in the annulus fibrosus, while in degenerated discs, cell clusters and disorganised fibres were observed in the nucleus pulposus. Highly fibrotic lamellae and interlamellar cells in the annulus fibrosus could be found in the degenerated discs. Layers distributed more irregularly with increased interbundle spaces, and the loss of distinct layers resulted in reduced ability to response to loads (Fig. 4).

Disc height index

MRI analysis revealed significant narrowing of the intervertebral space two weeks after induction of IVDD. No change of DHI could be found in the control group from week zero to week ten.

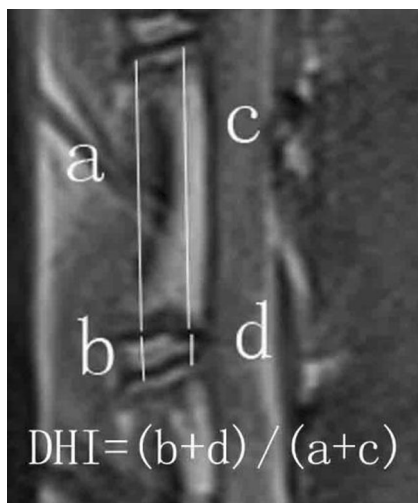


Fig. 2 Representative axial MRI image of a rabbit disc and the measurement protocol yielding the disc height index (DHI)

Table 2 Oligonucleotide primers for RT-PCR analysis

Gene	Gene symbol	Forward primer	Reverse primer
Glyceraldehyde-3-phosphate dehydrogenase	GAPDH	TCACCATCTTCCAGGAGCGA	CACAATGCCGAAGTGGTCGT
Aggrecan	ACAN	TCTACCGCTGCGAGGTGAT	TGTAATGGAACACGATGCCTTT
Collagen, type II, alpha 1	COL2A1	GGAAGAGTGGAGACTACTGGATTGAC	TCCATGTTGCAGAAAACCTTCA

The mean DHI in PBS and sham groups continued decreasing during follow-up, and there was no significant difference between the two groups. The mean DHI in the PBS group decreased to 82.98 ± 4.33 %, 74.06 ± 3.87 % and 68.86 ± 3.84 % at weeks two, six and ten, respectively, when compared with that of the control group. However, the DHI in the BMSCs group decreased to 84.55 ± 4.25 %, 80.82 ± 4.32 % and 78.45 ± 3.64 % at weeks two, six and ten, respectively (Table 3), and decreased more slowly than that in PBS and sham groups, especially at week ten after transplantation ($P < 0.05$, Fig. 5).

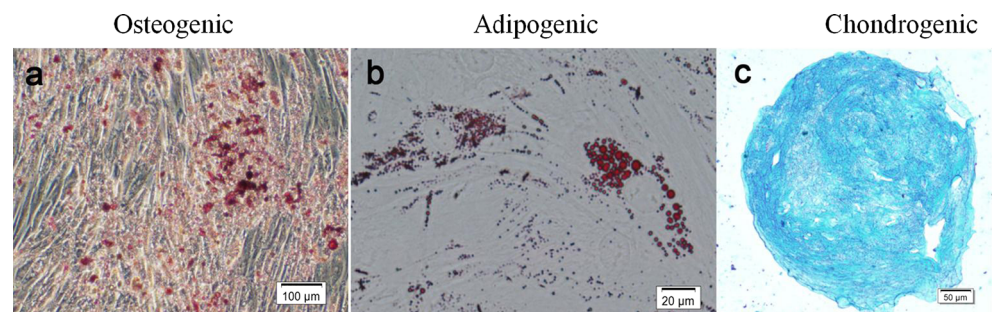
T2 signal intensity

MRI showed a significant decrease in T2-weighted signal intensity of the nucleus pulposus at week zero, which is the same as results in humans with IVDD. Comparisons among groups were made at weeks two, six and ten after cell transplantation. The MRI T2-weighted signal intensity of the nucleus pulposus in BMSCs, PBS and sham groups decreased significantly two weeks after disc stabbing, and the signal intensity was restored partially after cell transplantation only in the BMSCs group (Fig. 6).

T2 relaxation time

The T2 relaxation time of the nucleus pulposus decreased significantly in PBS and sham groups after induction of IVDD. The mean T2 relaxation time of the nucleus pulposus in the control group was ~ 150 ms, which decreased after stabbing to 83.25 ± 18.46 ms two weeks later ($P < 0.01$), and then plateaued. In contrast, BMSC transplantation resulted in a significant increase in T2 relaxation time. This value was 96.62 ± 10.49 ms, 109.97 ± 13.34 ms and 133.62 ± 10.04 ms at weeks two, six and ten, respectively (Fig. 7).

Fig. 3 a–c Osteogenic, chondrogenic and adipogenic differentiation of BMSCs



The T2 relaxation time did not differ between PBS and sham groups at weeks two, six and ten. When the data in these two groups were compared to that in the BMSCs group, no significant difference could be found at week two. However, there were significant differences seen at weeks six and ten ($P < 0.05$, $P < 0.01$, respectively).

Comparisons within each group were made at weeks zero, two, six and ten. Within the PBS and the sham groups, no statistical difference was found at weeks zero, two, six and ten. There was a statistical difference with an F value of 13.46 and $P < 0.01$ within the BMSCs group.

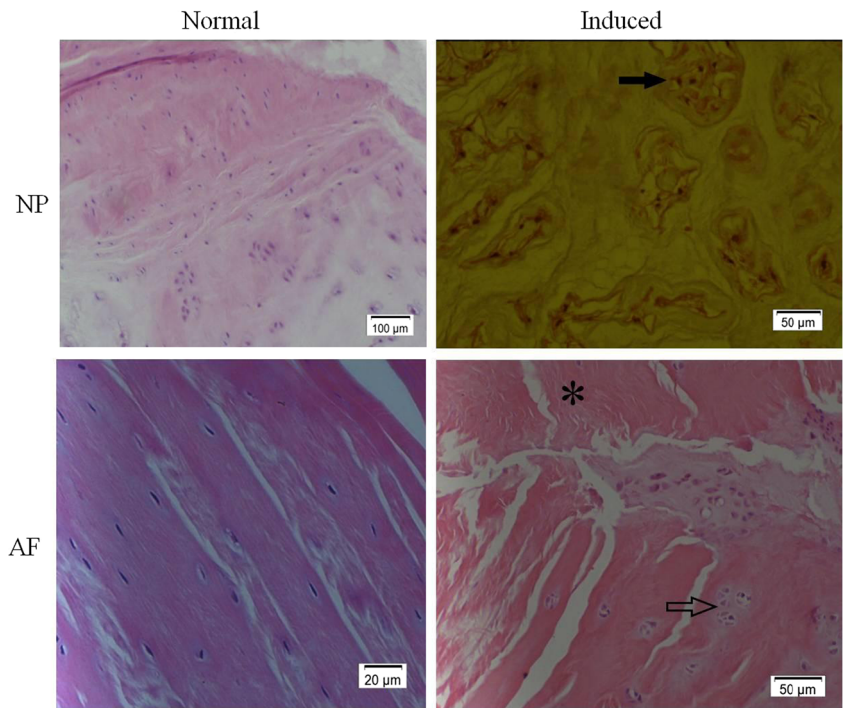
Real-time RT-PCR of matrix-specific genes

Analysis of the expression of matrix-specific genes showed lower *ACAN* and *COL2A1* gene expression in degenerated nucleus pulposus when compared to the normal nucleus ($P < 0.01$ and $P < 0.05$, respectively). After BMSC transplantation, expression of *ACAN* and *COL2A1* gradually increased (Figs. 8 and 9).

Comparisons among groups were made at the same time points. It was shown that *ACAN* expression did not differ between PBS and sham groups at weeks zero, two, six and ten. When the data in these two groups were compared with that in the BMSCs group, no significant differences were apparent at weeks zero and two, while statistical differences developed at weeks six and ten ($P < 0.01$, $P < 0.01$, respectively). Similarly, *COL2A1* gene expression did not differ between PBS and sham groups at weeks zero, two, six and ten. When the data from the two groups were compared to that of the BMSCs group, it was shown that *COL2A1* expression gradually increased, but there was no significant difference until week ten ($P < 0.05$).

Comparisons within each group were made at weeks zero, two, six and ten. Both *ACAN* and *COL2A1* expression in the

Fig. 4 Morphology of discs. In the control group, cells were distributed regularly in the nucleus pulposus (NP) and annulus fibrosus (AF). In the degenerated discs, cell clusters and disorganised fibres were observed in the nucleus pulposus (solid arrow on upper right). Disorganised fibres (asterisk on lower right) and interlamellar GAG matrix (hollow arrow on lower right) were noted in the degenerated annulus fibrosus



BMSCs group had statistical differences with an *F* value of 35.09 and *P*<0.01 and an *F* value of 7.704 and *P*<0.01, respectively. Within the PBS and sham groups, no statistical difference could be found.

Correlation analysis between T2 relaxation time and the expression levels of matrix-specific genes

In general, T2 relaxation time and the gene expression of *ACAN* and *COL2A1* were positively correlated ($R^2=0.9278$, *P*<0.01; $R^2=0.7211$, *P*<0.01, respectively), during follow-up after BMSC transplantation (Fig. 10).

Discussion

The normal IVD was rich in extracellular matrix which consisted of a well-organised framework of macromolecules that attracted and retained water [26]. Water and extracellular matrix content in IVD decreased upon aging and degeneration

Table 3 Decrease in DHI (%) at weeks 0, 2, 6 and 10 after transplantation

Group	Week 0	Week 2	Week 6	Week 10
BMSCs group	89.44±4.16	84.55±4.25	80.82±4.32	78.45±3.64
PBS group	87.56±4.20	82.98±4.33	74.06±3.87	68.86±3.84
Sham group	87.34±3.79	81.75±4.02	75.90±4.37	67.38±4.47
Control group	99.85±3.26	98.79±3.05	99.44±3.54	98.23±3.36

[27]. This study and previous studies indicated that BMSC-based therapy may be effective for disc and other tissue regeneration, as demonstrated by histological and pathological means in the laboratory and measurement of T2-weighted image signal intensities in clinical settings [11, 12, 28–31]. However, laboratory detection methods were invasive and signal intensity could not be measured in absolute terms for a number of reasons, including problems with signal detection and amplification [32]. Thus, we evaluated the efficiency of absolute T2 value as a non-invasive means of detecting reconstruction of the nucleus pulposus.

MRI is commonly used in the clinical setting for examination of the degeneration of bone, cartilage and other tissues. T2 mapping could be used to quantify the water content and

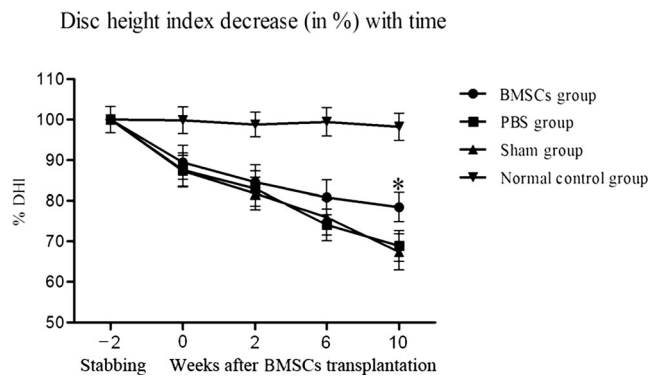


Fig. 5 MRI analysis revealed significant narrowing of the disc space two weeks after stabbing. The disc height in BMSCs, PBS and sham groups gradually decreased after stabbing. A significant difference between BMSCs and PBS groups was apparent at week ten (*P*<0.05), suggesting that BMSCs could slow down the degeneration of discs

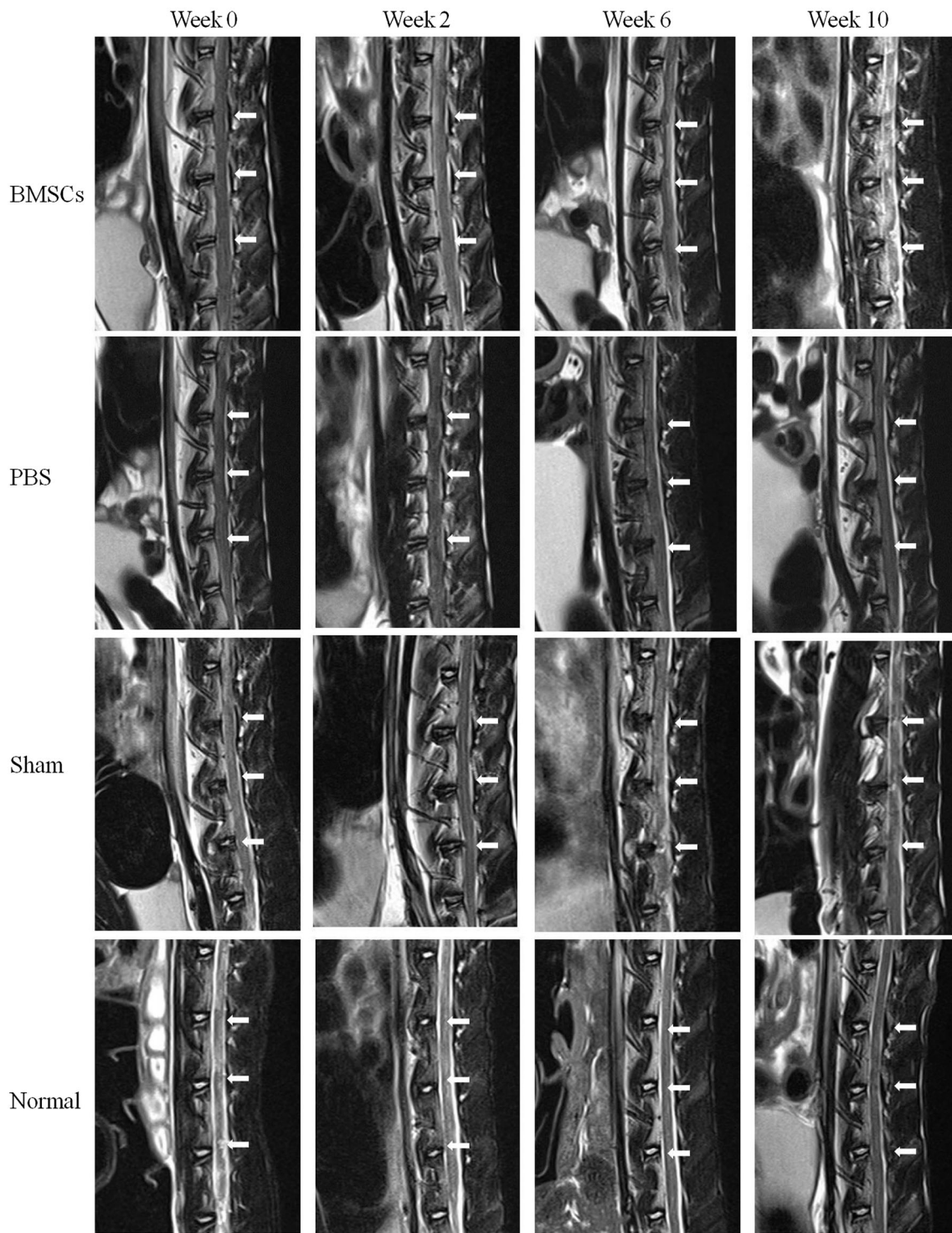


Fig. 6 The MRI T2-weighted signal intensities of the nucleus pulposus in BMSCs, PBS and sham groups all decreased significantly at the time of transplantation (two weeks after disc stabbing), and only those of the MSCs group gradually increased after cell transplantation

identify early-stage cartilage abnormality and IVDD [16, 18, 33–35]. T2 relaxation time is the decay constant of MRI T2 signal intensity, and it is not dependent on imaging parameters. T2 relaxation time, an intrinsic property of tissue, can reflect the molecular environment of tissues,

especially the water and matrix contents [16]. The main curative effect of stem cell transplantation therapy is to promote and renew the production of extracellular matrix [28]. Thus, T2 mapping might be a promising method to reflect the water and matrix content in

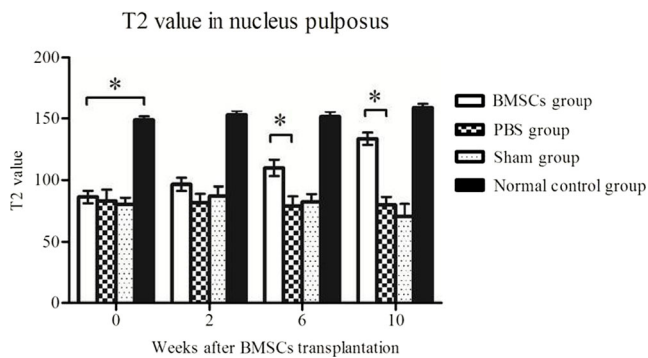


Fig. 7 The T2 relaxation time of the nucleus pulposus decreased significantly in PBS and sham groups after induction of IVDD. In contrast, BMSC transplantation resulted in a significant increase in T2 relaxation time. The T2 relaxation time did not differ between PBS and sham groups at weeks two, six and ten. When the data from the two groups were compared to those of the BMSCs group, no significant difference was apparent at week two. However, significant differences developed at weeks six and ten ($P < 0.05$, $P < 0.01$, respectively). Values are presented as means \pm SD ($n = 3$ per group)

tissues, especially to evaluate disc regeneration after BMSC transplantation.

We found that *COL2* and *ACAN* gene expression decreased in the degenerated disc, but increased after BMSC transplantation. At week six, the gene expression in the BMSCs group was significantly higher than that in the PBS group. Similarly, the T2 values decreased after disc stabbing, which might reflect the reduction in extracellular matrix and water content [36], but increased significantly after BMSC transplantation.

The disc height in both BMSCs and PBS groups gradually decreased after stabbing. No significant difference was apparent between BMSCs and PBS groups until week ten, suggesting that BMSCs could slow down the degeneration of discs.

T2 relaxation time and the gene expression of *ACAN* and *COL2* were positively correlated. *ACAN* expression increased

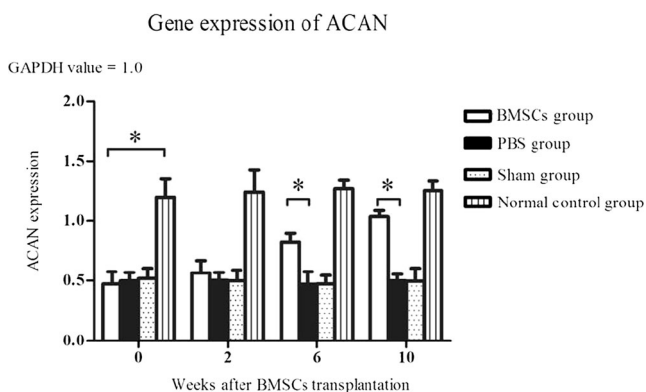


Fig. 8 Analysis of the expression levels of matrix-specific genes showed that as compared to the normal nucleus, *ACAN* gene expression levels were significantly lower in degenerated nucleus pulposus ($P < 0.01$). The expression levels of *ACAN* in PBS and sham groups did not differ significantly. Comparisons between BMSCs and PBS groups indicated that *ACAN* gene expression significantly differed both at weeks six and ten ($P < 0.01$ for both). Values are presented as means \pm SD ($n = 3$ per group)

Gene expression of COL2A1

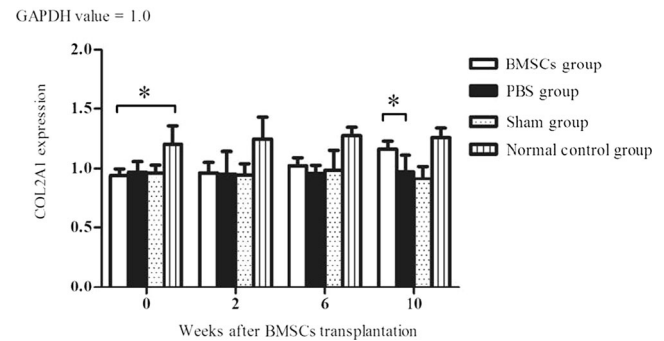
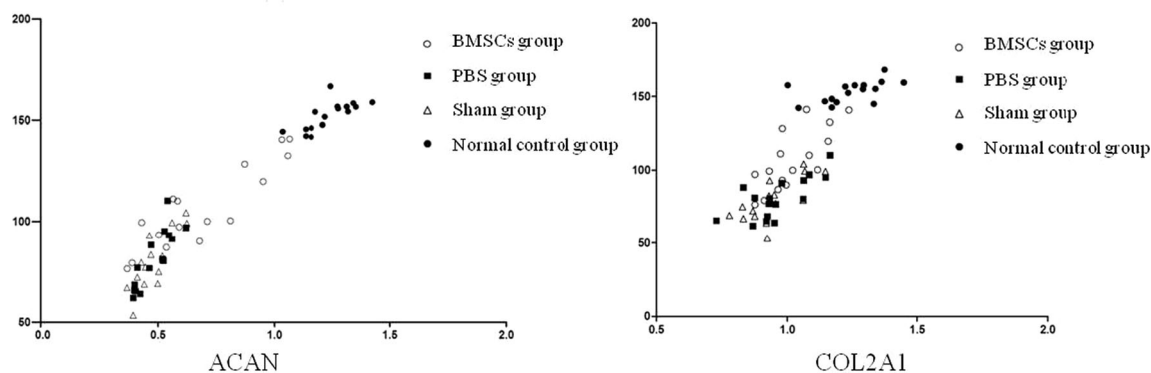


Fig. 9 Analysis of the expression levels of matrix-specific genes showed that as compared to the normal nucleus, *COL2A1* gene expression levels were significantly lower in the degenerated nucleus pulposus ($P < 0.01$). The expression levels of *COL2A1* in PBS and sham groups did not differ significantly. Comparisons between BMSCs and PBS groups indicated that *COL2A1* gene expression was significantly different until week ten (week 6: $P = 0.22$, week 10: $P < 0.05$). Values are presented as means \pm SD ($n = 3$ per group)

more significantly and earlier, whereas *COL2* expression increased later. Also, the calculated R^2 between the *ACAN* expression in the nucleus pulposus and T2 relaxation time was 0.9278, which is greater than that between T2 relaxation time and *COL2* expression (0.7211). Thus, the T2 value correlated with *ACAN* expression more obviously than *COL2* expression. The reason might be that *ACAN* absorbs more water than *COL2* does, contributing more water content in the disc. The other reason was that the expression of *ACAN* is much greater than that of *COL2* in the nucleus pulposus [37]. Similar results could be found in a study of calf and human cadaver discs, in which the T2 relaxation time of the whole disc was correlated with proteoglycan content with an R^2 value of 0.859 [16]. The difference in our study was that T2 mapping was used to evaluate the extracellular matrix re-establishment in IVDD after BMSC transplantation in an animal model.

T2 mapping may be used in the future to evaluate the disc regeneration process. Firstly, the T2 relaxation time is highly correlated with *ACAN* expression and *ACAN* is the principal component of the matrix of the nucleus pulposus. We firstly showed that the T2 relaxation time of the nucleus increased as *ACAN* expression arose after BMSC transplantation. *ACAN* synthesis indicates repair taking place in the nucleus pulposus. Secondly, T2 mapping is non-invasive and has greater advantages over other methods of detecting matrix content in vivo. It is very difficult to visualise disc regeneration after therapy in the clinical setting, which is a limitation of translating biological therapy from the laboratory to the clinic. Finally, T2 mapping could yield absolute values stably. T2 relaxation time is an intrinsic property of tissue and reflects the molecular environment. The data vary less than T2 signal intensities and exhibit minimal measurement bias. It may be easy to examine disc regeneration in this manner.

Correlations for T2 relaxation time with ACAN and COL2A1 expression



Group	ACAN expression Vs. T2 relaxation time			COL2 expression Vs. T2 relaxation time		
	n	R ²	p	n	R ²	p
BMSCs group	16	0.7855	< 0.0001*	16	0.5448	0.0011*
PBS group	16	0.7127	< 0.0001*	16	0.5293	0.0014*
Sham group	16	0.7045	< 0.0001*	16	0.5475	0.0010*
Normal control group	16	0.5454	0.0011*	16	0.2819	0.0343*
Total	48	0.9278	< 0.0001*	48	0.7211	< 0.0001*

*Significant correlations have a p value less than or equal to 0.05.

Fig. 10 T2 relaxation time and the expression levels of *ACAN* and *COL2A1* were strongly correlated ($R^2=0.9278$, $P<0.01$; $R^2=0.7211$, $P<0.01$, respectively), during follow-up after BMSC transplantation

This study is the first to evaluate the disc degeneration and regeneration process using T2 mapping, a sensitive and non-invasive detection means, developed in a rabbit model. What is more, T2 values can be used to define regeneration stages quantitatively. T2 mapping could be used to evaluate the disc degeneration and regeneration process and might be used to detect other diseases, such as infection. Recently, studies suggested that a dormant infection was involved in disc degeneration, though some researchers had different opinions [38–48]. An infection in a disc must result in inflammatory processes and tissue oedema in the early period. The question is whether T2 mapping could be used to detect the water and other molecular changes in inflammatory processes non-invasively. If it is possible, T2 mapping can provide suggestions of injection regardless of contamination and show what exactly happens in patients with disc herniation who have not been operated on.

In summary, T2 values decreased in the degenerating nucleus pulposus of the rabbit and might be used to reflect the decrease in matrix and water contents. BMSC transplantation partly reversed disc degeneration, which indicated the efficiency of stem cells in the treatment of spine degeneration. T2 values increased as *ACAN* levels rose in the nucleus pulposus. Thus, T2 mapping may be used to non-invasively evaluate the regeneration of nucleus sensitively. We defined regeneration stages using quantitative data. In conclusion, T2 mapping of

IVD matrix and water contents may be useful for diagnosis of degenerative disc diseases and evaluation of treatment efficiency in the clinical setting.

Acknowledgments The work was supported by the National Natural Science Foundation of China (81272035; 81071493; 81201423) and the 51st China Postdoctoral Science Foundation 2012 (2012 M511800). Thanks to Prof. Ling Qin (The Chinese University of Hong Kong) for language editing. Thanks to Yuan-cheng Wang (Southeast University) for MRI evaluation.

References

- Dagenais S, Caro J, Haldeman S (2008) A systematic review of low back pain cost of illness studies in the United States and internationally. *Spine J* 8:8–20
- Sakai D (2008) Future perspectives of cell-based therapy for intervertebral disc disease. *Eur Spine J* 17(Suppl 4):452–458
- Phillips FM, Reuben J, Wetzel FT (2002) Intervertebral disc degeneration adjacent to a lumbar fusion. An experimental rabbit model. *J Bone Joint Surg Br* 84:289–294
- Rui YF, Lui PP, Lee YW, Chan KM (2012) Higher BMP receptor expression and BMP-2-induced osteogenic differentiation in tendon-derived stem cells compared with bone-marrow-derived mesenchymal stem cells. *Int Orthop* 36:1099–1107
- Tsai MT, Lin DJ, Huang S, Lin HT, Chang WH (2012) Osteogenic differentiation is synergistically influenced by osteoinductive treatment and direct cell-cell contact between murine osteoblasts and mesenchymal stem cells. *Int Orthop* 36:199–205

6. Mueller MB, Blunk T, Appel B, Maschke A, Goepferich A, Zellner J, Englert C, Prantl L, Kujat R, Nerlich M, Angele P (2013) Insulin is essential for in vitro chondrogenesis of mesenchymal progenitor cells and influences chondrogenesis in a dose-dependent manner. *Int Orthop* 37:153–158
7. Qin L (2013) Translational medicine in orthopaedics. *J Orthop Transl* 1:3–5
8. Ciapetti G, Granchi D, Devescovi V, Leonardi E, Greggi T, Di Silvestre M, Baldini N (2012) Ex vivo observation of human intervertebral disc tissue and cells isolated from degenerated intervertebral discs. *Eur Spine J* 21(Suppl 1):S10–S19
9. Roughley P, Martens D, Rantakokko J, Alini M, Mwale F, Antoniou J (2006) The involvement of aggrecan polymorphism in degeneration of human intervertebral disc and articular cartilage. *Eur Cell Mater* 11:1–7, discussion 7
10. Longo UG, Papapietro N, Petrillo S, Franceschetti E, Maffulli N, Denaro V (2012) Mesenchymal stem cell for prevention and management of intervertebral disc degeneration. *Stem Cells Int* 2012: 921053
11. Sakai D, Mochida J, Yamamoto Y, Nomura T, Okuma M, Nishimura K, Nakai T, Ando K, Hotta T (2003) Transplantation of mesenchymal stem cells embedded in Atelocollagen gel to the intervertebral disc: a potential therapeutic model for disc degeneration. *Biomaterials* 24: 3531–3541
12. Sakai D, Mochida J, Iwashina T, Watanabe T, Nakai T, Ando K, Hotta T (2005) Differentiation of mesenchymal stem cells transplanted to a rabbit degenerative disc model: potential and limitations for stem cell therapy in disc regeneration. *Spine (Phila Pa 1976)* 30:2379–2387
13. Terti M, Paaajanen H, Laato M, Aho H, Komu M, Komano M (1991) Disc degeneration in magnetic resonance imaging. A comparative biochemical, histologic, and radiologic study in cadaver spines. *Spine (Phila Pa 1976)* 16:629–634
14. Antoniou J, Pike GB, Steffen T, Baramki H, Poole AR, Aebi M, Alini M (1998) Quantitative magnetic resonance imaging in the assessment of degenerative disc disease. *Magn Reson Med* 40:900–907
15. Nightingale T, MacKay A, Pearce RH, Whittall KP, Flak B (2000) A model of unloaded human intervertebral disk based on NMR relaxation. *Magn Reson Med* 43:34–44
16. Marinelli NL, Haughton VM, Muñoz A, Anderson PA (2009) T2 relaxation times of intervertebral disc tissue correlated with water content and proteoglycan content. *Spine (Phila Pa 1976)* 34:520–524
17. Niu G, Yang J, Wang R, Dang S, Wu EX, Guo Y (2011) MR imaging assessment of lumbar intervertebral disk degeneration and age-related changes: apparent diffusion coefficient versus T2 quantitation. *AJNR Am J Neuroradiol* 32:1617–1623
18. Takashima H, Takebayashi T, Yoshimoto M, Terashima Y, Tsuda H, Ida K, Yamashita T (2012) Correlation between T2 relaxation time and intervertebral disk degeneration. *Skeletal Radiol* 41:163–167
19. Trattnig S, Stelzener D, Goed S, Reissegger M, Mamisch TC, Paternostro-Sluga T, Weber M, Szomolanyi P, Welsch GH (2010) Lumbar intervertebral disc abnormalities: comparison of quantitative T2 mapping with conventional MR at 3.0 T. *Eur Radiol* 20:2715–2722
20. Welsch GH, Mamisch TC, Hughes T, Zilkens C, Quirbach S, Scheffler K, Kraff O, Schweitzer ME, Szomolanyi P, Trattnig S (2008) In vivo biochemical 7.0 Tesla magnetic resonance: preliminary results of dGEMRIC, zonal T2, and T2* mapping of articular cartilage. *Invest Radiol* 43:619–626
21. Dunn TC, Lu Y, Jin H, Ries MD, Majumdar S (2004) T2 relaxation time of cartilage at MR imaging: comparison with severity of knee osteoarthritis. *Radiology* 232:592–598
22. Menezes NM, Gray ML, Hartke JR, Burstein D (2004) T2 and T1rho MRI in articular cartilage systems. *Magn Reson Med* 51:503–509
23. Kern S, Eichler H, Stoeve J, Klüter H, Bieback K (2006) Comparative analysis of mesenchymal stem cells from bone marrow, umbilical cord blood, or adipose tissue. *Stem Cells* 24:1294–1301
24. Sobajima S, Shimer AL, Chadderton RC, Kompel JF, Kim JS, Gilbertson LG, Kang JD (2005) Quantitative analysis of gene expression in a rabbit model of intervertebral disc degeneration by real-time polymerase chain reaction. *Spine J* 5:14–23
25. Lu DS, Shono Y, Oda I, Abumi K, Kaneda K (1997) Effects of chondroitinase ABC and chymopapain on spinal motion segment biomechanics. An in vivo biomechanical, radiologic, and histologic canine study. *Spine (Phila Pa 1976)* 22:1828–1834, discussion 1834–1825
26. Longo UG, Ripalda P, Denaro V, Forriol F (2006) Morphologic comparison of cervical, thoracic, lumbar intervertebral discs of cynomolgus monkey (*Macaca fascicularis*). *Eur Spine J* 15:1845–1851
27. Krueger EC, Perry JO, Wu Y, Haughton VM (2007) Changes in T2 relaxation times associated with maturation of the human intervertebral disk. *AJNR Am J Neuroradiol* 28:1237–1241
28. Yang F, Leung VY, Luk KD, Chan D, Cheung KM (2009) Mesenchymal stem cells arrest intervertebral disc degeneration through chondrocytic differentiation and stimulation of endogenous cells. *Mol Ther* 17:1959–1966
29. Chiu EJ, Newitt DC, Segal MR, Hu SS, Lotz JC, Majumdar S (2001) Magnetic resonance imaging measurement of relaxation and water diffusion in the human lumbar intervertebral disc under compression in vitro. *Spine (Phila Pa 1976)* 26:E437–E444
30. Xie XH, Wang XL, He YX, Liu Z, Sheng H, Zhang G, Qin L (2012) Promotion of bone repair by implantation of cryopreserved bone marrow-derived mononuclear cells in a rabbit model of steroid-associated osteonecrosis. *Arthritis Rheum* 64:1562–1571
31. Wang X, Wang Y, Gou W, Lu Q, Peng J, Lu S (2013) Role of mesenchymal stem cells in bone regeneration and fracture repair: a review. *Int Orthop* 37:2491–2498
32. Watanabe A, Benneker LM, Boesch C, Watanabe T, Obata T, Anderson SE (2007) Classification of intervertebral disk degeneration with axial T2 mapping. *AJR Am J Roentgenol* 189:936–942
33. Stelzener D, Kovacs BK, Goed S, Welsch GH, Hirschfeld C, Paternostro-Sluga T, Friedrich KM, Mamisch TC, Trattnig S (2012) Effect of short-term unloading on T2 relaxation time in the lumbar intervertebral disc—in vivo magnetic resonance imaging study at 3.0 tesla. *Spine J* 22:257–264
34. Friedrich KM, Shepard T, de Oliveira VS, Wang L, Babb JS, Schweitzer M, Regatte R (2009) T2 measurements of cartilage in osteoarthritis patients with meniscal tears. *AJR Am J Roentgenol* 193:W411–415
35. Mosher TJ, Dardzinski BJ (2004) Cartilage MRI T2 relaxation time mapping: overview and applications. *Semin Musculoskelet Radiol* 8: 355–368
36. Zou J, Yang H, Miyazaki M, Morishita Y, Wei F, McGovern S, Wang JC (2009) Dynamic bulging of intervertebral discs in the degenerative lumbar spine. *Spine (Phila Pa 1976)* 34:2545–2550
37. Minogue BM, Richardson SM, Zeef LA, Freemont AJ, Hoyland JA (2010) Characterization of the human nucleus pulposus cell phenotype and evaluation of novel marker gene expression to define adult stem cell differentiation. *Arthritis Rheum* 62:3695–3705
38. Albert HB, Sorensen JS, Christensen BS, Manniche C (2013) Antibiotic treatment in patients with chronic low back pain and vertebral bone edema (Modic type 1 changes): a double-blind randomized clinical controlled trial of efficacy. *Eur Spine J* 22:697–707
39. Albert HB, Lambert P, Rollason J, Sorensen JS, Worthington T, Pedersen MB, Nørgaard HS, Vemallis A, Busch F, Manniche C, Elliott T (2013) Does nuclear tissue infected with bacteria following disc herniations lead to Modic changes in the adjacent vertebrae? *Eur Spine J* 22:690–696

40. Aebi M (2013) Is low back pain after disc herniation with Modic type 1 changes a low-grade infection? *Eur Spine J* 22:689
41. Aebi M (2013) The two papers of Hanne Albert et al. about Modic I changes of the vertebra published in the *European Spine Journal* of April 2013. Editorial. *Eur Spine J* 22:1693
42. Ahmad Z, Rai A, Donell S, Crawford R (2013) Letter to the editor concerning: “Antibiotic treatment in patients with chronic low back pain and vertebral bone edema (Modic type 1 changes): a double-blind randomized controlled trial of efficacy” by Albert HB et al. *Eur Spine J* (2013) 22:697–707. *Eur Spine J* 22:2344–2345
43. Almefty KK, Turner JD, Theodore N (2013) From narcotics to antibiotics: evolving concepts in the treatment of lower back pain. *World Neurosurg* 80:442–443
44. Dean BJ (2013) Do these results apply to the ‘intervention naive’ patient? *Eur Spine J* 22:1702
45. Sotto A, Dupeyron A (2013) Letter to the editor concerning: “Antibiotic treatment in patients with chronic low back pain and vertebral bone edema (Modic type 1 changes): a double-blind randomized controlled trial of efficacy” by Albert HB et al. *Eur Spine J* 22:697–707. *Eur Spine J* 22:1704–1705
46. O’Dowd J, Casey A (2013) Antibiotics a cure for back pain, a false dawn or a new era? *Eur Spine J* 22:1694–1697
47. Shubhakaran K, Khichar RJ (2013) Backache and infection. *Eur Spine J* 22:2348
48. Lings S (2014) Antibiotics for low back pain? *Eur Spine J* 23:469–472